International Journal of Mechanical and Production Engineering Research and Development (IJMPERD)
ISSN (P): 2249-6890; ISSN (E): 2249-8001
Vol. 9, Issue 3, Jun 2019, 1455-1468

MODE I INTERLAMINAR FRACTURE TOUGHNESS AND FRACTOGRAPHIC OBSERVATION OF MULTIDIRECTIONAL CARBON FIBER/EPOXY COMPOSITES

MUHAMAD FAUZIABDRASED & SUNG HO YOON*

Department of Mechanical Engineering, Kumoh National Institute of Technology, Gumi, South Korea

ABSTRACT

Mode I interlaminar fracture toughness was evaluated and fracture surfaces were observed to investigate crack propagation behaviors and establish the relationship between fracture toughness and fracture surface morphology in multidirectional carbon fiber/epoxy composites. Double cantilever beam specimens, with artificial cracks made of Teflon film embedded in the middle plane, were prepared. Six crack lengths were considered (25–50 mm). The slopes of the load displacement curves depend on the initial crack length. The mode I interlaminar fracture toughness at crack initiation is approximately constant, regardless of the initial crack length, but fluctuates with crack propagation. The fracture surface morphology indicates that the R-curve is closely related to the crack propagation mechanism. The fracture surface exhibits damage, such as crack migration, fiber bridging, crack branching, double cracking, and ply splits. These results provide insight into interlaminar fracture toughness assessment and the crack propagation behavior of multidirectional carbon fiber/epoxy composites.

KEYWORDS: Multidirectional Carbon Fiber/Epoxy Composites, Interlaminar Fracture Toughness, Fracture Surface Morphology, Initial Crack Length & Crack Propagation Behavior

Received: Apr 19, 2019; **Accepted:** May 09, 2019; **Published:** Jun 08, 2019; **Paper Id.:** IJMPERDJUN2019153

Original Article

1. INTRODUCTION

Significant advances in composite materials have resulted in a marked increase in applications where lightweight and low-density materials, as well as high strength, stiff, and tough materials, are required. Carbon fiber/epoxy composites are one of the most commonly used materials in advanced applications, including the aerospace, automotive, and maritime industries, and sporting goods. Their material properties are significantly influenced by the fiber orientation and stacking sequence of the constituents, which can be tailored to the intended purpose of advanced structural applications. However, one of the shortcomings is that laminated composites do not reinforce in the thickness direction, and delamination tends to occur readily. Delamination is one of the most common failures in laminated composites and occurs readily in the so-called mode I opening mode.

Delamination has received significant attention from numerous researchers [1-5]. Standardization of ASTM D 5528 [6] and ISO 15024 [7], using double cantilever beam specimens, were proposed to evaluate the mode I interlaminar fracture toughness of unidirectional laminated composites. Multidirectional laminated composites are preferred over unidirectional laminated composites, and are a form that is applied in practice to obtain intended material properties by changing the fiber orientation and stacking sequence. Because delamination occurs readily in multidirectional laminated composites, it is necessary to quantitatively and/or qualitatively

evaluate the mode I interlaminar fracture toughness.

The load increases significantly after the onset of crack initiation because the damage, such as fiber bridging, crack migration, and double cracking in multidirectional laminated composites, results in a significant increase in the interlaminar fracture toughness. Moura et al. [1] reported that mode I interlaminar fracture toughness at crack propagation, when the bridging fiber was cut and made free of fiber bridging, was similar to the value at crack initiation when fiber bridging was present. Pereira et al. [2] reported that mode I interlaminar fracture toughness of multidirectional laminated composites was four times greater than that of unidirectional laminated composites because of fiber bridging. In addition, interlaminar fracture toughness was increased because of fiber bridging when the crack propagated.

As fiber bridging has a significant effect on interlaminar fracture behavior, an appropriate method is required to quantitatively evaluate the interlaminar fracture toughness of multidirectional laminated composites. Measuring the interlaminar fracture toughness of unidirectional laminated composites can be used to effectively determine that of multidirectional laminated composites. Regarding interlaminar fracture behavior, a number of studies in which various specimens were tested have been reported recently. Huddar et al. [8] reported the effect of initial crack length on mode I interlaminar fracture toughness of glass fiber/epoxy laminated composites. They observed that the interlaminar fracture toughness at crack initiation increased with increasing initial crack length. Shokrieh et al. [9] reported that mode I interlaminar fracture toughness is approximately constant regardless of the initial crack length. In addition, some researchers reported that mode I interlaminar fracture toughness of multidirectional laminated composites had a pronounced plateau, even as the crack propagated [10, 11]. Therefore, the aim of this study is to evaluate mode I interlaminar fracture toughness of multidirectional carbon fiber/epoxy laminated composites with varying initial crack lengths. In addition, the damage mechanism is investigated by observing fracture surface morphology as the crack propagates.

2. EXPERIMENT

2.1. Procedure

Double cantilever beam specimens were obtained from laminated composites by stacking carbon fiber/epoxy prepregs in the desired sequence. The stacking sequence was $[0_2/\pm50/0_2/\pm50//0/\pm50/0_2/\pm50/0_2]$, where // represents a thin Teflon film inserted into the middle layer for crack formation. The specimens were all cut with a diamond-coated blade to ensure a suitable initial crack length. Six initial crack lengths, ranging from 25 mm to 50 mm, were used, and five specimens were tested for each crack length. The configuration of the specimens is shown in Figure 1 and the dimensions are presented in Table 1.

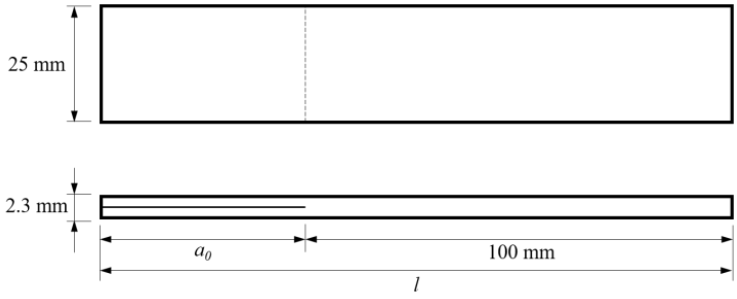

Figure 1: Configuration of the Specimens

Table 1: Dimension of the specimens

Crack Length (mm)	Specimen Length (mm)
25	125
30	130
35	135
40	140
45	145
50	150

The test was conducted in accordance with the procedure in ASTM D 5528 [6]. The specimen with the loading block was mounted on the test fixture of a Zwick/Z100 universal testing machine, as shown in Figure 2. The load was applied at a crosshead speed of 2 mm/min until the crack propagated from 2 mm to 5 mm, and was then unloaded back to zero. The crack propagation length and behavior were accurately measured and observed, respectively, using an optical traveling microscope at a magnification of 100x. This process was repeated until the overall crack propagation length was approximately 50 mm.

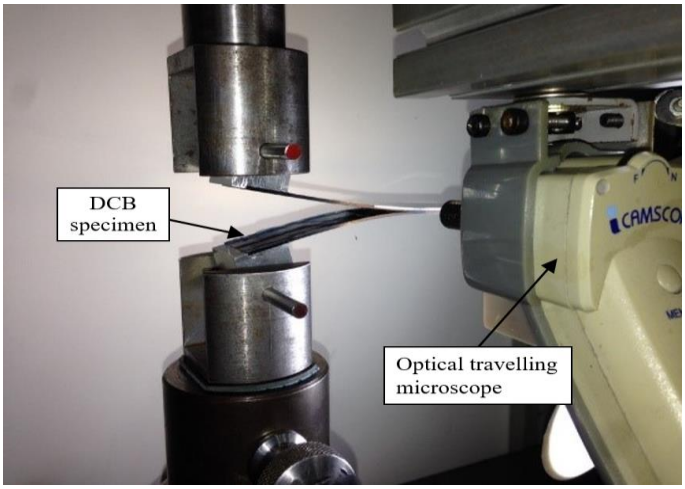

Figure 2: Experimental Set-Up for Interlaminar Fracture Toughness

2.2. Data Reduction Method

Three of the methods for determining mode I interlaminar fracture toughness are the modified beam theory, compliance calibration, and modified compliance calibration methods. All three methods provide similar results for unidirectional and multidirectional laminated composites [12]. However, ASTM recommends the modified beam theory method to obtain the most conservative values.

The strain energy release rate is derived based on the simple beam theory:

$$G_{IC} = \frac{3P\delta}{2ba} \tag{1}$$

Where P is the load, δ is the load point displacement, b is the specimen width, and a is the crack length. However, equation (1) applies only to fully fixed specimens at the crack tip and does not consider fiber bridging and loading block geometry. Because this equation does not provide reliable results, the modified beam theory method of equation (2) proposed by ASTM is applied.

$$G_{IC} = \frac{3P\delta}{\left(2b\left(a+|\Delta|\right)\right)} \tag{2}$$

where Δ is a calibration parameter that reflects the effect of test conditions, such as the loading block and the rotation of the crack tip. This parameter can be determined by generating a plot of the cube root of compliance, $C^{1/3}$, for the crack length a, and is the absolute value of the intercept of the horizontal axis of the $C^{1/3}$-a plot, as shown in Figure 3.

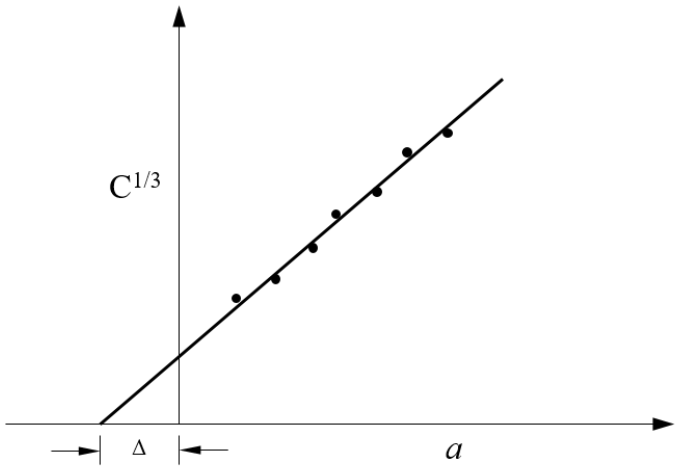

Figure 3: Determination of Δ in the Modified Beam Theory

2.3. Fracture Surface Morphology

The fracture surface was examined using an optical traveling microscope and a scanning electron microscope (SEM) (JSM 7601F, JEOL, Japan). After the test, a diamond-coated blade was used to cut the specimen and a thin platinum coating was applied to the fracture surface. Scanning electron microscopy was performed at 200x, 500x, 1000x, and 3000x magnification to investigate the damage mechanism of the fracture surface.

3. RESULTS AND DISCUSSIONS

3.1. Load–Displacement Curve

Figure 4 shows a typical load–displacement curve for the specimen with an initial crack length of 35 mm. Loading and unloading were repeatedly applied to the specimen to obtain the load–displacement curve. Points that deviate from the linear slope of the load–displacement curve were considered as the starting points of cracks during the calculations, and the interlaminar fracture toughness was determined using the load and displacement when the crack occurred in each sequence.

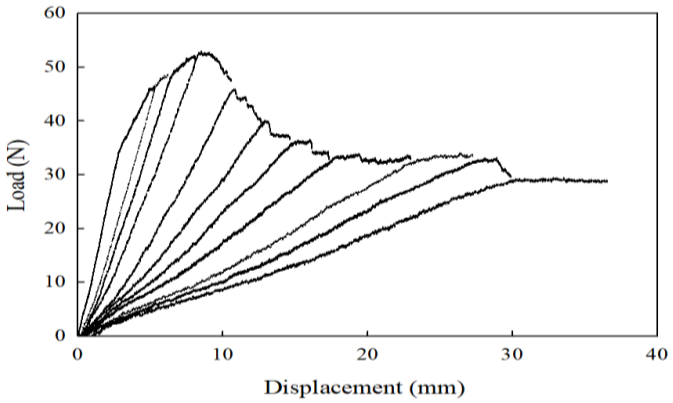

Figure 4: Typical Load-Displacement Curve for the Specimen with an Initial Crack Length of 35 mm

Figure 5 shows the typical load–displacement curves for six specimens with initial crack lengths of 25 mm, 30 mm, 35 mm, 40 mm, 45 mm, and 50 mm. The gradients of the load–displacement curves depend on the flexural rigidity of the specimens and on the initial crack length, and the gradient decreases as the initial crack length increases. When the initial crack length is 25 mm, the slope is the steepest and the flexural rigidity is the highest. As anticipated, the shorter the initial crack length, the steeper the slope.

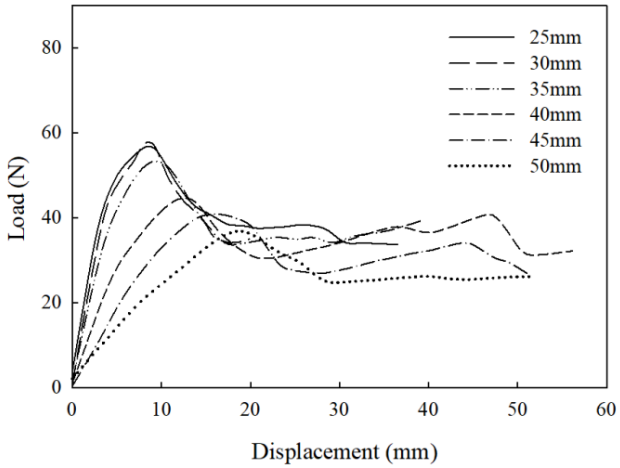

Figure 5: Typical Load-Displacement Curves for Six Specimens with Initial Crack Lengths of 25 mm, 30 mm, 35 mm, 40 mm, 45 mm, and 50 mm

When the load is applied and the crack is propagated, the slope of the load – displacement curve appears linear until the crack initiates, and then exhibits nonlinearities when the crack propagates. This is observed on all specimens after crack initiation. Figure 6(a) shows the observed stair-shaped crack propagation at the edge of the specimen. Cracks penetrate into the -50° ply located below the initial crack plane, resulting in stair-shaped crack propagation. Figure 6(b) shows fiber bridging as the crack propagates. When this damage occurs, the load will increase significantly as the crack propagates. This type of damage was also reported in other studies of multidirectional laminated composites [5, 11].

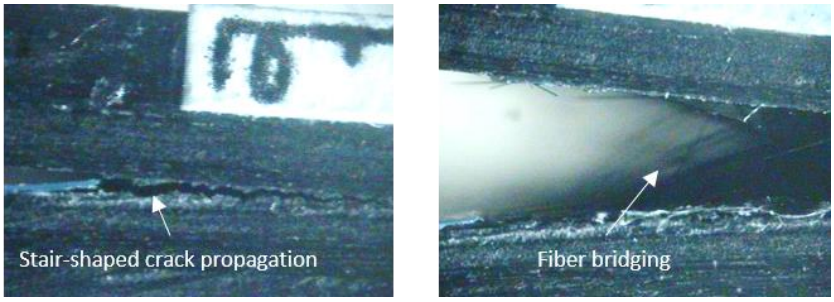

Figure 6: Observation of Stair-Shaped Crack Propagation and Fiber Bridging

Figure 7 shows the damage observed at the edge of the specimen through the mode I test. If the crack continues to propagate, other damage, including crack jump, stair-shaped crack propagation, double cracking, and crack branching, could typically be observed. As the crack propagates, there is a marginal increase and decrease in the load. For instance, in the case of a specimen with an initial crack of 40 mm, the load is repeatedly increased and decreased gradually once the load reaches its maximum value, as shown in Figure 5. In this case, even if the load is increased, no further cracks are observed at the edge of the specimen; however, increasing the load will cause the cracks to propagate unstably.

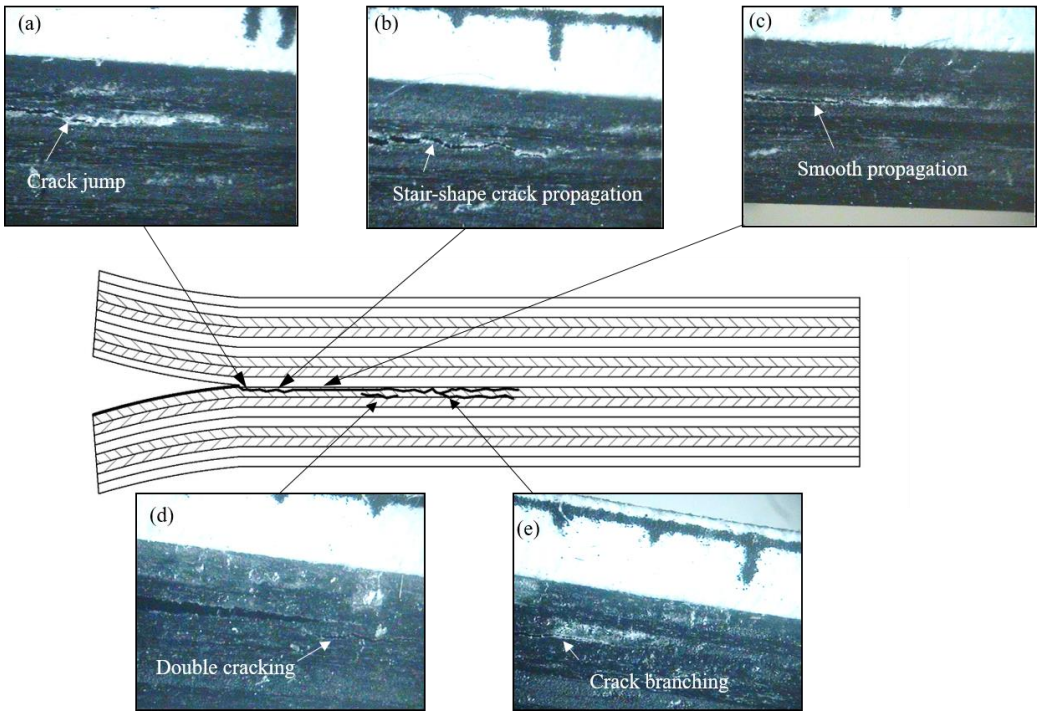

Figure 7: Damage Observed at the Edge of the Specimen: (a) Crack Jump, (b) Stair-Shaped Crack Propagation, (c) Smooth Propagation, (d) Double Cracking and (e) Crack Branching

3.2. R-Curve

Figure 8 shows the load–displacement curve and its *R*-curve representing the relationship between fracture toughness and crack length. When the crack initiates, as shown in Figure 8(a), the fracture toughness is determined at a point deviating from the linear slope of the loading curve of the first load–displacement curve, and the fracture toughness during crack propagation is determined at a point deviating from the linear slope of the load action curve in the remaining load–displacement curves. As shown in Figure 8(b), when the crack propagates, the fracture toughness is higher than the fracture toughness at the initiation of the crack, and the crack propagates and gradually decreases as the crack progresses.

This difference is affected by the condition of the crack tip. Typically, artificial crack tips, which are formed with resin pockets, have a dominant effect on the resin at crack initiation. As the crack propagates, bridging fibers increase. Interlaminar fracture toughness at crack propagation is higher than at crack initiation. Fiber bridging helps improve interlaminar fracture toughness because it prevents cracks from forming fracture surfaces. Similar results have been reported in other studies [4, 5].

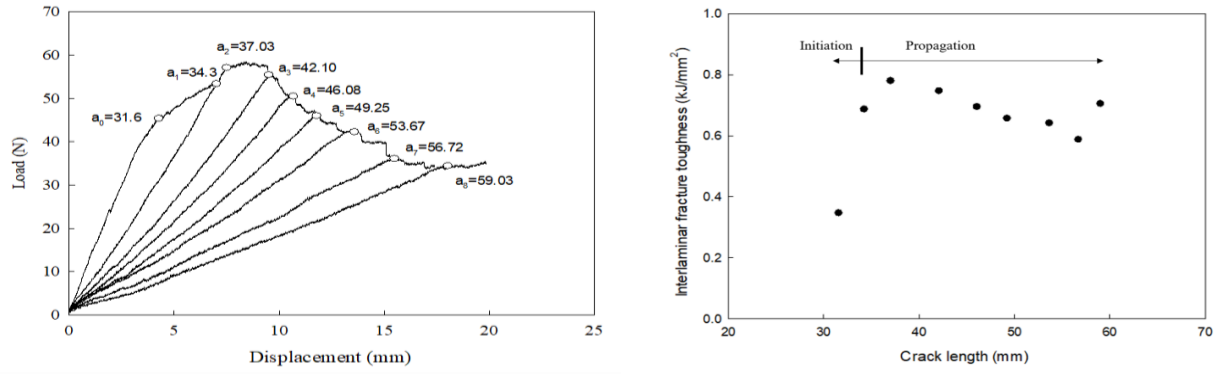

(a) Load-Displacement Curves **(b) R-curve**

Figure 8: Relationship between Fracture Toughness and Crack Length

Figure 9 shows the *R*-curve for the crack lengths of specimens for different initial crack lengths, and Table 2 summarizes the interlaminar fracture toughness of these specimens. Mode I interlaminar fracture toughness at crack initiation is shown to be approximately 0.3 kJ/m^2, and is not significantly affected by the initial crack length. This means that the interlaminar fracture toughness at crack initiation is approximately constant. However, if the crack propagates, the interlaminar fracture toughness of the six specimens with different initial crack lengths indicates an increase in crack length. As discussed, this increase is because of fiber bridging as the crack propagates. Results indicate that interlaminar fracture toughness is affected by damage and the fracture process; other damage, including crack migration, stair-shaped propagation, double cracking, and crack branching, is also observed.

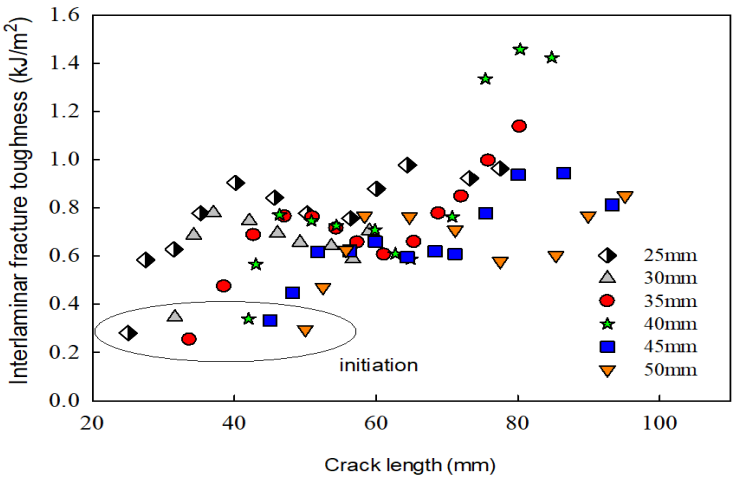

Figure 9: R-Curve for the Crack Lengths of Specimens for Different Initial Crack Lengths

Table 2: Interlaminar Fracture Toughness at Initiation and Propagation

Initial Crack Length (mm)	Interlaminar Fracture Toughness(kJ/mm^2)		
	Initiation	Propagation	(S.D)
25	0.28	0.82	(0.12)
30	0.34	0.69	(0.06)
35	0.25	0.76	(0.17)
40	0.35	0.85	(0.28)
45	0.33	0.70	(0.15)
50	0.29	0.68	(0.12)

The damage process because of crack propagation affects the trends of the *R*-curves. This can be observed in Figure 10, where the interlaminar fracture toughness after the crack initiates decreases as the crack propagates, and then increases as the crack propagates further. From the edge of the specimen, it can be seen that double cracking decreases the interlaminar fracture toughness, as shown in Figure 10(b), and intense fiber bridging increases the interlaminar fracture toughness, as shown in Figure 10(c). In particular, fiber bridging increases as the crack propagates, specifically after double cracking. This fiber bridging prevents delamination from occurring continuously, which increases the interlaminar fracture toughness. This damage requires a higher load to propagate the crack, therefore, it increases the interlaminar fracture toughness. These observations indicate that damage to multidirectional laminated composites has a significant effect on the interlaminar fracture toughness.

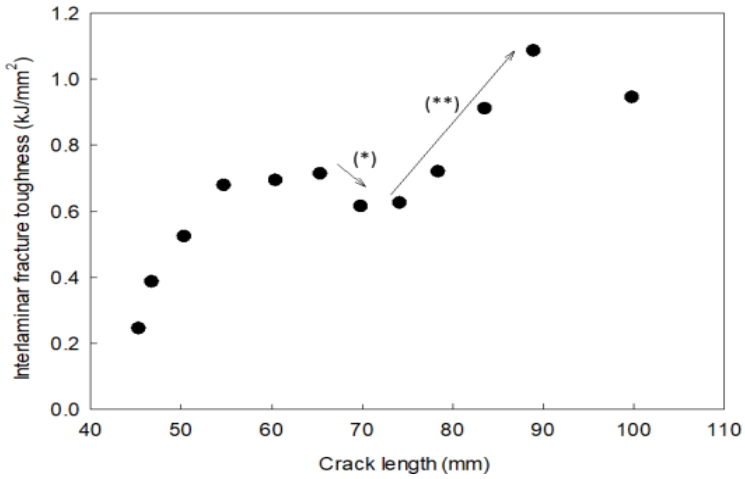

(a) Trends of R-curves

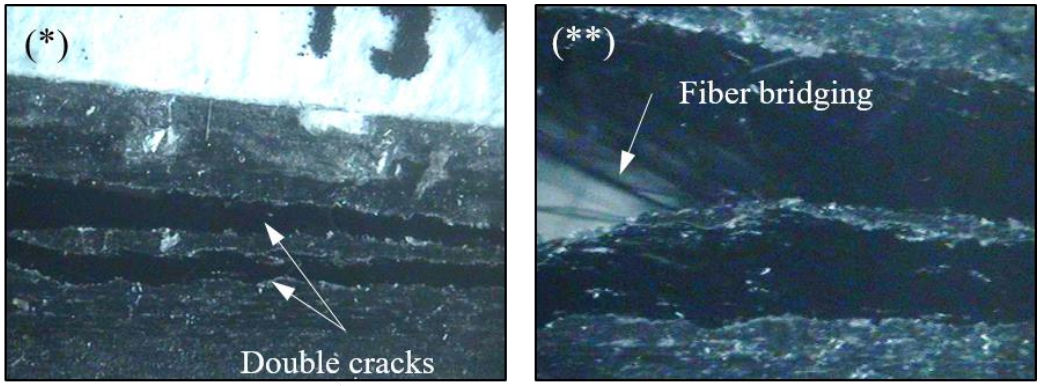

(b) Damage Process

Figure 10: Trends of R-curves and Damage Process

4. FRACTOGRAPHIC ANALYSIS ON DELAMINATION SURFACE

4.1. Fracture Surface Analysis

The fracture surface was analyzed using a microscope and SEM to study the crack propagation mechanism, including crack migration, stair-shaped crack propagation, and double cracking. Figures 11(a) and 12(a) show the fracture surfaces of the upper and lower parts of the specimen, respectively. Regardless of the initial crack length, the patterns of the fracture surfaces are similar and the -50° ply is covered at the front of the fracture surface. An initial artificial crack made from Teflon film is located on the interface of [0/-50] and moves to the lower -50° ply when the crack is initiated. Other studies have reported that, as the crack propagates, it moves to adjacent plies [13-16]. This occurs because the energy required to propagate the crack through the migration is significantly lower than the energy required to propagate along the existing crack plane [14].

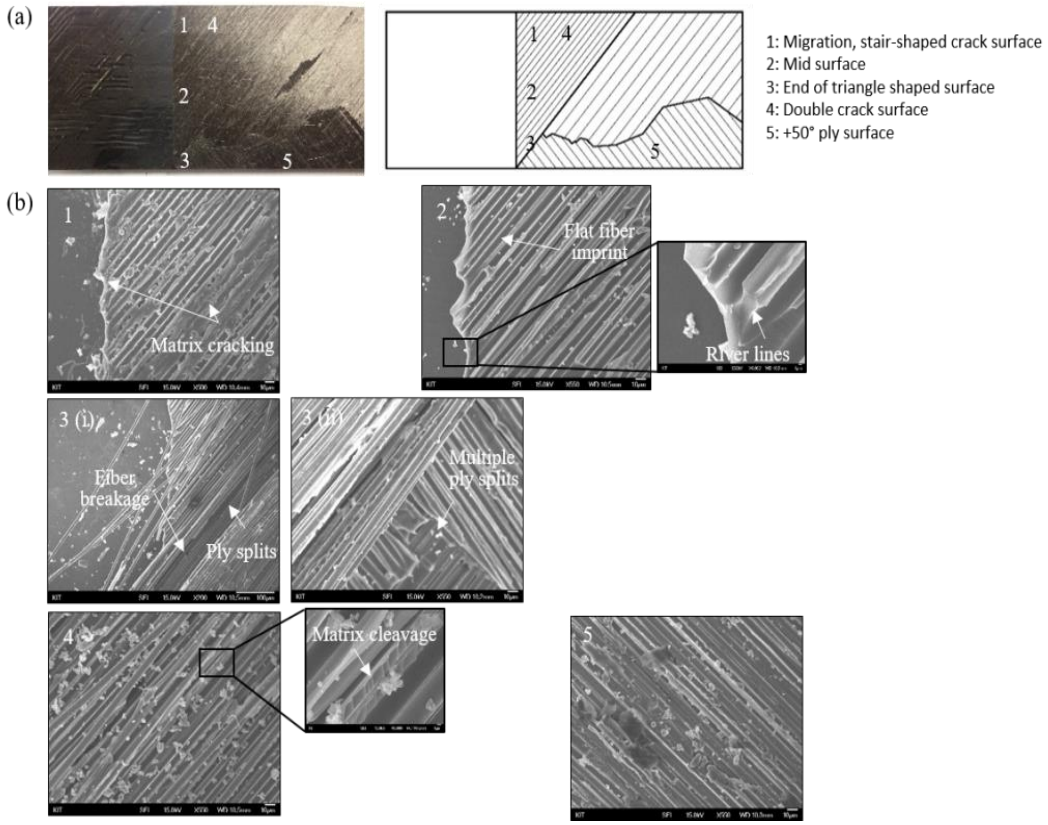

Figure 11: Fracture Surface Analysis: (a) Observed Locations in the Upper Fracture Surface of the Specimen and (b) SEM Images of Each Point

Stair-shaped cracks and double cracking are the primary factors for investigating fracture mechanism when the crack propagates, and SEM analyses have observed specific locations where such phenomena occur. Figure 11(a) shows the observed locations in the upper fracture surface of the specimen, as designated by points 1 to 5. Figure 11(b) shows the SEM images of each point shown in Figure 11(a). Figure 12 shows the observed locations in the lower fracture surface of the specimen corresponding to the locations shown in Figure 11, and the SEM images at the corresponding points 1 to 5.

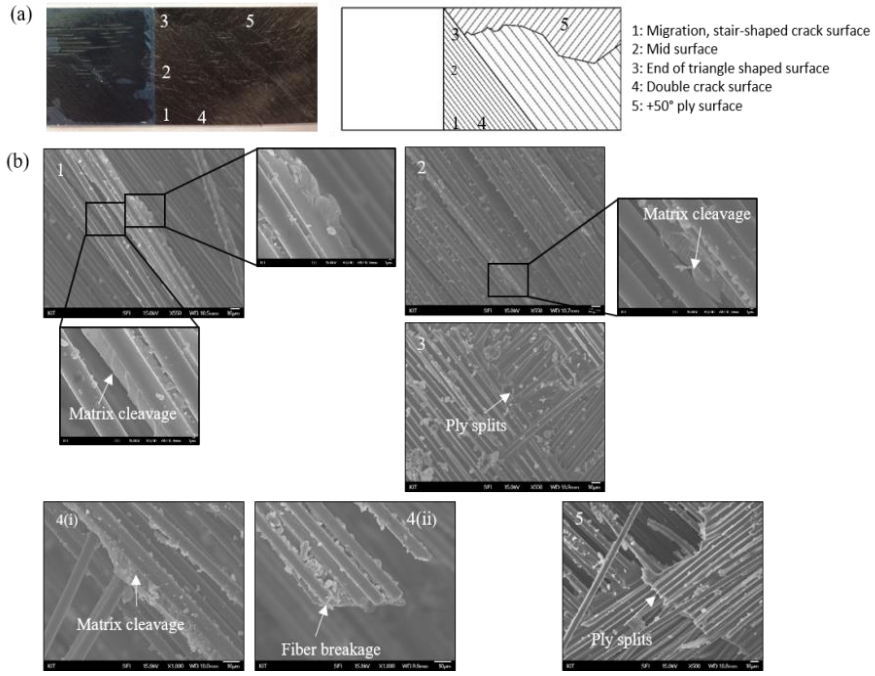

Figure 12: Fracture Surface Analysis: (a) Observed Locations in the Lower Fracture Surface of the Specimen and (b) SEM Images of Each Point

The pattern of the fracture surface at point 1, where crack migration and stair-shaped crack propagation are indicated, is dominant with matrix cracks of -50° ply. Typical mode I fracture surface phenomena, including matrix cleavage and fiber debonding from the matrix, are observed. It is noted that the epoxy matrix remaining in the fiber exhibits significant resin deformation as the fiber leaves the matrix, indicating that the adhesion between the fiber and resin is satisfactory. This is associated with fiber bridging, which causes multiple damage mechanisms in the interface between the fiber and the matrix. Points 2 and 3 are the center and the rear edges of the surface, respectively. The SEM images at the two points show a fracture pattern with matrix cleavage and fiber imprints across the surface, which are similar to the pattern in point 1. However, at point 3, ply split occurs, resulting in +50° ply exposure below the surface of the -50° ply. Ply split affects the crack propagation and causes delamination of adjacent ply interfaces at certain points. Double cracking appears at point 4. The SEM image at this point shows that the fibers are separated from the matrix, and the fiber breakage is observed because of double cracking. Observation of separated fibers in the matrix shows that the epoxy matrix is partially covered in the fiber. At point 5, it is indicated that delamination occurs at the rear edge of the specimen at the +50° ply. In the +50° ply fracture surface, fiber imprint, matrix cleavage, and ply splits are observed, and appear as fracture patterns similar to the -50° ply fracture surface.

4.2. Relationship between Fracture Surface Morphology and Load–Displacement Curve

Figure 13 shows the relationship between fracture surface morphology and load–displacement curves. As shown in Figure 13(a), the fracture surface is divided into three regions, denoted A, B, and C. Region A is covered with a thick layer of -50° ply, B with +50° ply, and C with a thin layer of -50° ply. Three phases were defined to correlate the fracture surface morphology with the load–displacement curve. Phase 1 is the stage at which the crack initiates, phase 2 is where a thin layer of -50° ply is formed, and phase 3 is where the triangular thick layer of -50° ply ends.

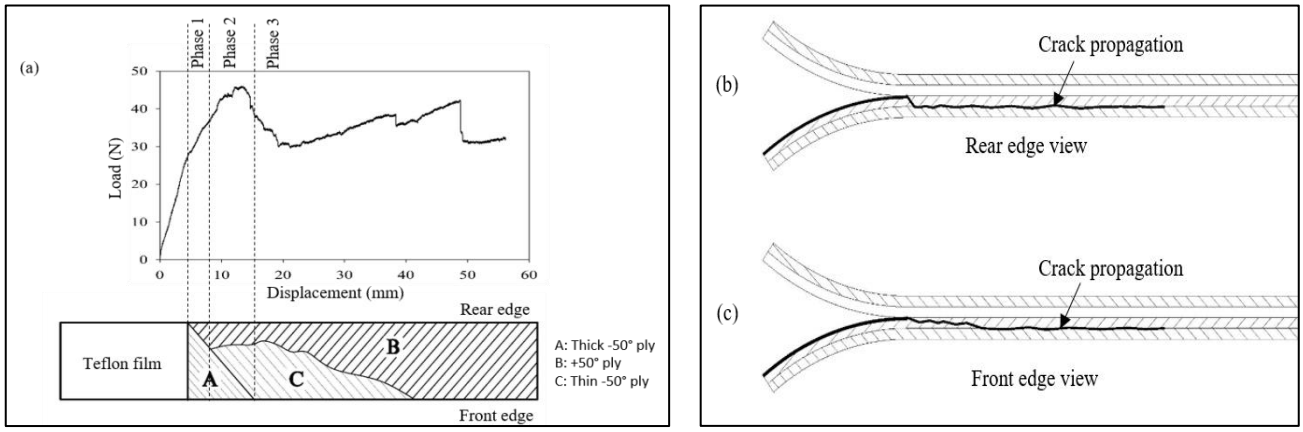

Figure 13: Relationship between Fracture Surface Morphology and Load-Displacement Curves: (a) Fracture Surface with Load-Displacement Curves (b) Delamination Path at Rear Edge and (c) Delamination Path at Front Edge

In phase 1 of Figure 13(a), the crack initiates at the crack tip and propagates to form a triangular-shaped fracture surface on region A and part of region B. The triangular-shaped surface of region A is not a delamination at the [0/-50] interface, but is a fracture in the -50° ply. This triangular-shaped surface is typically observed in the crack propagation of angle ply laminated composites [3, 16]. In phase 1, the crack initiates from a point that deviates from the linear slope of the load–displacement curve and the load gradually increases, even when the crack propagates. This increase in load is closely related to crack migration and fiber bridging. After passing through the fracture surface in phase 1, the crack propagates toward the -50° ply, forming a thin layer of -50° ply in the fracture surface. Phase 2 shows both regions A and B, as well as region C. Observing the load–displacement curve, there is no abrupt change in the slope, and this pattern continues until the load exceeds the maximum value. From this observation, the fracture surface morphology does not significantly affect the load–displacement curve, and shows that the load is applied even if it decreases after reaching its maximum value. The maximum load is not affected by the propagated crack length, but by the amount of fiber bridging. Moura et al. [1] reported similar results that fiber bridging had a significant effect on the load of the load–displacement curve. As in phase 2, the fracture surface morphology does not affect the load of the load–displacement curve in phase 3. The load of the load–displacement curve continues to decrease as the displacement increases, even after phase 3 begins, as shown in Figure 13. This observation shows that the triangular-shaped layer of -50° ply does not affect the load–displacement trend.

However, if the crack continues to propagate, damage such as double cracking, as shown in Figure 10(b), will reduce the load. As reported in other studies [3, 13], crack wandering is related to the energy absorption mechanism. Fiber bridging increases the energy needed for the fracture, which increases the maximum load. Double cracking decreases the energy required for the fracture, which causes the maximum load to be small.

Another important observation in this study is the stick-slip phenomenon. Even if the load is increased to a certain level, the crack does not propagate; however, above that level, the crack propagates unstably. This phenomenon is common at the point where cracks and transverse fibers intersect in multidirectional laminated composites [17]. Observation of the fracture surface shows that several fracture patterns occurred. Multiple ply splits occur at the interface of [50/-50] and [-50/0], as shown in Figure 14. These crack migrations and multiple ply splits result in unstable crack propagation.

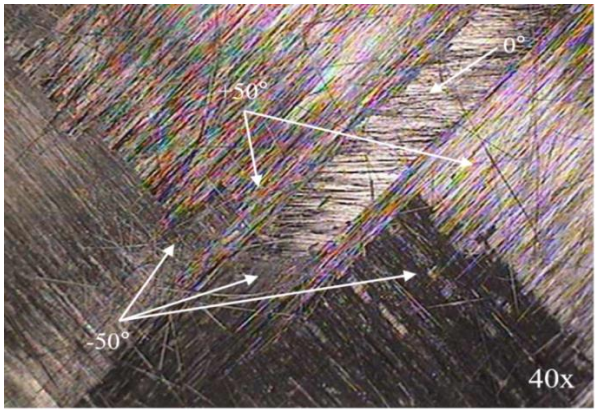

Figure 14: Fracture Surface Morphology with Multiple Ply Splits at the Interface of [50/-50] and [-50/0]

5. CONCLUSIONS

In order to investigate the crack initiation and propagation behavior of multidirectional carbon fiber/epoxy laminated composites, the interlaminar fracture toughness was investigated and a fracture surface analysis was performed. Mode I interlaminar fracture toughness tests were conducted by preparing double cantilever beam specimens with five initial crack lengths. It could be seen that the linear slopes of the load–displacement curves varied with the initial crack lengths. The linear slopes, closely related to the flexural rigidity of the specimen, steepened with decreasing initial crack length. The *R*-curve indicated that the interlaminar fracture toughness did not increase or decrease with initial crack length at crack initiation. However, as the crack propagated, the interlaminar fracture toughness was greater than that at crack initiation, and varied as the crack propagated. This was because the fiber bridging, double cracking, and stick-slip phenomena were affected.

To obtain the relationship between the crack propagation mechanism and the fracture surface morphology, the fracture surface was analyzed as the crack propagated. Although the initial crack length varied, the fracture surface morphology was similar, therefore, the crack propagation behavior did not differ. In order to investigate the relationship between the fracture surface morphology and the load in the load–displacement curves, the curves were divided into three distinct regions. The fracture surface morphology in each region was a satisfactory reflection of the respective interlaminar fracture toughness.

The information obtained from this study could be useful for evaluating the interlaminar fracture toughness and investigating crack propagation behavior in multidirectional carbon fiber/epoxy laminated composites.

6. ACKNOWLEDGMENTS

We acknowledge the financial support for this study by the Kumoh National Institute of Technology.

REFERENCES

1. *M. F. S. F. Moura, R.D.S.G. Campilho, A.M. Amaro, and P.N.B. Reis, Interlaminar and intralaminar fracture characterization of composites under mode I loading, CompositeStructures92(2010)144–149.*
2. *A.B. Pereira and A.B. de Morais, Mode I interlaminar fracture of carbon/epoxy multidirectional laminates, Composite Science and Technology 64 (2004) 2261-2270.*
3. *P.Naghipour, M. Bartsch, L. Chernova, J. Hausmann, and H. Voggenreiter, Effect of fiber angle orientation and stacking sequence on mixed mode fracture toughness of carbon fiber reinforced plastics: Numerical and experimental investigations, Materials Science and Engineering A527(2010)509–517.*
4. *N.S. Choi, A.J. Kinloch, and J.G. Williams, Delamination Fracture of Multidirectional Carbon-Fiber/Epoxy Composite under Mode I, ModeII and Mixed-Mode I/II Loading, Journal of Composite Materials 33 (2004) 73–100.*
5. *T.A. Sebaey, N. Blanco, J. Costa, and C.S. Lopes, Characterization of crack propagation in mode I delamination of multidirectional CFRP laminates, Composite Science and Technology72(2012)1251–1256.*
6. *ASTM D 5528-01, Standard Test Method for Mode I Interlaminar Fracture Toughness of Unidirectional Fiber-Reinforced Polymer Matrix Composites, ASTM International.*
7. *ISO 15024, Fibre-reinforced plastic composites - Determination of mode I interlaminar fracture toughness, GIC, for unidirectionally reinforced materials.*
8. *A. Huddhar, A. Desai, C.M. Sharanaprabhu, S.K. Kudari, and P.S.S. Gouda, Studies on effect of pre-crack length variation on Inter-laminar fracture toughness of a Glass Epoxy laminated composite, IOP Conference Series: Materials Science and Engineering 149,2016.*
9. *M.M. Shokrieh, M. Salamat-Talab, and M. Heidari-Rarani, Effect of initial crack length on the measured bridging law of unidirectional E-glass/epoxy double cantilever beam specimens, Materials and Design 55(2014) 605–611*
10. *L. Yao, R. Alderliesten, M. Zhao, and R Benedictus, Bridging effect on mode I fatigue delamination behavior in composite laminates, Composite Part A 63 (2014) 103-109.*
11. *Y. Gong, L. Zhao, J. Zhang, Y. Wang, and N. Hu, Delamination propagation criterion including the effect of fiber bridging for mixed-mode I/II delamination in CFRP multidirectional laminates, Composite Science and Technology 151 (2017) 302–309.*
12. *X.J.Gong, A. Hurez, and G. Verchery, On the determination of delamination toughness by using multidirectional DCB specimens, Polymer Testing 29 (2010) 658–666.*
13. *E.S. Greenhalgh, C. Rogers, and P. Robinson, Fractographic observations on delamination growth and the subsequent migration through the laminate, Composites Science and Technology 69(2009) 2345–2351.*
14. *M.F. Pernice, N.V. de Carvalho, J.G. Ratcliffe, and S.R. Hallett, Experimental study on delamination migration in composite laminates, Composite Part A 73 (2015) 20-34.*
15. *Prabhu, P. G., Kumar, C. A., Pandiyaraj, R., Rajesh, P., & Kumar, L. S. (2014). Study on utilization of waste PET bottle fiber in concrete. Dimension (mm), 1, 17.*
16. *L. Zhao, Y. Wang, J. Zhang, Y. Gong, Z. Lu, N. Hu, and J. Xu, An interface-dependent model of plateau fracture toughness in multidirectional CFRP laminates under mode I loading, Composites PartB 131(2017) 196–208.*

17. *B.W. Kim and A.H.Mayer, Influence of fiber direction and mixed-moderatioon delaminate on fracture toughness of carbon/epoxy laminates, Composites Science and Technology 63(2003) 695–713.*
18. *F. Ozdil and L.A. Carlsson, Beam analysis of angle-ply laminate DCB specimens, Composites Science and Technology 59(1999) 305–315.*